

See discussions, stats, and author profiles for this publication at: <https://www.researchgate.net/publication/280102810>

# Ligand Accessibility and Bioactivity of a Hormone-Dendrimer Conjugate Depend on pH and pH History

ARTICLE *in* JOURNAL OF THE AMERICAN CHEMICAL SOCIETY · JULY 2015

Impact Factor: 12.11 · DOI: 10.1021/jacs.5b05952 · Source: PubMed

CITATION

1

READS

108

## 8 AUTHORS, INCLUDING:



**Zeynep Madak Erdogan**

University of Illinois, Urbana-Champaign

24 PUBLICATIONS 745 CITATIONS

SEE PROFILE



**Sung Chul Bae**

University of Illinois, Urbana-Champaign

103 PUBLICATIONS 1,673 CITATIONS

SEE PROFILE



**John A Katzenellenbogen**

University of Illinois, Urbana-Champaign

510 PUBLICATIONS 21,625 CITATIONS

SEE PROFILE

Article

## Ligand Accessibility and Bioactivity of a Hormone-Dendrimer Conjugate Depend on pH and pH History

Sung Hoon Kim, Zeynep Madak-Erdogan, Sung Chul Bae, Kathryn E. Carlson, Christopher G. Mayne, Steve Granick, Benita S. Katzenellenbogen, and John A Katzenellenbogen

*J. Am. Chem. Soc.*, **Just Accepted Manuscript** • DOI: 10.1021/jacs.5b05952 • Publication Date (Web): 17 Jul 2015

Downloaded from <http://pubs.acs.org> on July 21, 2015

### Just Accepted

"Just Accepted" manuscripts have been peer-reviewed and accepted for publication. They are posted online prior to technical editing, formatting for publication and author proofing. The American Chemical Society provides "Just Accepted" as a free service to the research community to expedite the dissemination of scientific material as soon as possible after acceptance. "Just Accepted" manuscripts appear in full in PDF format accompanied by an HTML abstract. "Just Accepted" manuscripts have been fully peer reviewed, but should not be considered the official version of record. They are accessible to all readers and citable by the Digital Object Identifier (DOI®). "Just Accepted" is an optional service offered to authors. Therefore, the "Just Accepted" Web site may not include all articles that will be published in the journal. After a manuscript is technically edited and formatted, it will be removed from the "Just Accepted" Web site and published as an ASAP article. Note that technical editing may introduce minor changes to the manuscript text and/or graphics which could affect content, and all legal disclaimers and ethical guidelines that apply to the journal pertain. ACS cannot be held responsible for errors or consequences arising from the use of information contained in these "Just Accepted" manuscripts.



ACS Publications

# Ligand Accessibility and Bioactivity of a Hormone-Dendrimer Conjugate Depend on pH and pH History

Sung Hoon Kim<sup>1</sup>, Zeynep Madak-Erdogan<sup>2</sup>, Sung Chul Bae<sup>3</sup>, Kathryn E. Carlson<sup>1</sup>, Christopher G. Mayne<sup>1</sup>, Steve Granick<sup>3</sup>, Benita S. Katzenellenbogen<sup>2</sup>, John A. Katzenellenbogen<sup>1\*</sup>

1. Department of Chemistry
2. Department of Molecular and Integrative Physiology , University of Illinois at Urbana-Champaign, Urbana, Illinois 61801, USA
3. IBS Center for Soft and Living Matter and UNIST, Ulsan, South Korea 689-798

Address Correspondence to:

John A. Katzenellenbogen  
Department of Chemistry  
University of Illinois  
600 South Mathews Avenue  
Urbana, IL 61801, USA  
217 333 6310 jkatzene@illinois.edu

Submitted to: *Journal of the American Chemical Society*

**Key Words:** PAMAM dendrimer, estrogen receptor, estrogen-dendrimer conjugate, non-genomic gene expression, genomic gene expression, pH dependent estrogenic effect, proximity-ligated ER $\alpha$  and pMAPK complex, ER $\alpha$ -pMAPK complex, proximity ligation assay.

**Abstract:**

Estrogen conjugates with a polyamidoamine (PAMAM) dendrimer have shown remarkably selective regulation of the non-genomic actions of estrogens in target cells. In response to pH changes, however, these estrogen-dendrimer conjugates (EDCs) display a major morphological transition that alters the accessibility of the estrogen ligands that compromises the bioactivity of the EDC. A sharp break in dynamic behavior near pH 7 occurs for three different ligands on the surface of a PAMAM-G6 dendrimer: a fluorophore (tetramethylrhodamine, TMR) and two estrogens (17 $\alpha$ -ethynylestradiol and diphenolic acid). Collisional quenching and time-resolved fluorescence anisotropy experiments with TMR-PAMAM reveal high ligand shielding above pH 7 and low shielding below pH 7. Furthermore, when pH was cycled from 8.5 (conditions of ligand-PAMAM conjugation) to 4.5 (e.g., endosome/lysosome) and through 6.5 (e.g., hypoxic environment) back to pH 8.5, the 17 $\alpha$ -ethynylestradiol and diphenolic acid PAMAM conjugates experience a dramatic, irreversible loss in cell stimulatory activity; dynamic NMR studies indicate that the hormonal ligands had become occluded within the more hydrophobic core of the PAMAM dendrimer. Thus, the active state of these estrogen-dendrimer conjugates appears to be metastable. This pH-dependent irreversible masking of activity is of considerable relevance to the design of drug conjugates with amine-bearing PAMAM dendrimers.

**Keywords** PAMAM dendrimer, estrogen receptor, estrogen-dendrimer conjugate, non-genomic gene expression, genomic gene expression, pH dependent estrogenic effect, proximity-ligated ER $\alpha$  and pMAPK complex, ER $\alpha$ -pMAPK complex, proximity ligation assay.

## INTRODUCTION

Administration of exogenous estrogen agonists activates both extranuclear- and nuclear-initiated pathways of the estrogen receptor (ER) and results in global activation of ER in almost all target tissues. Because global activation of ER is often not clinically beneficial, a premium has been placed on the stimulation of ER activity in a tissue-selective manner.<sup>1</sup> One recently explored approach to this has involved pharmacologically altering the balance of ER activation through the extranuclear vs. nuclear signaling routes.<sup>2,3</sup> To activate selectively the extranuclear signaling pathway of ER, we designed and synthesized an “estrogen-dendrimer conjugate” (EDC) in which the estrogenic hormone, 17 $\alpha$ -ethynylestradiol (EE<sub>2</sub>), is attached covalently to a G6 PAMAM dendrimer (**Figure 1**).<sup>3,4</sup>

In cell-based and *in vivo* studies, EDC showed remarkable selectivity, activating cytoplasmic kinase cascades without direct nuclear action,<sup>2,3,5-10</sup> modulating dopamine receptor,<sup>10</sup> exerting neuroprotective effects,<sup>11</sup> regulating metabolic disease,<sup>12-14</sup> improving cortical bone mass,<sup>15</sup> participating in estrogen-mediated DNA repair,<sup>16</sup> and providing cardiovascular protection without stimulating reproductive organs (e.g., uterus) and breast cancers.<sup>6,17</sup> These results indicate that this polymer-based hormone conjugate, EDC, exhibits a novel form of selective ER activation: Because of its size, EDC cannot enter the nucleus, and thus cannot activate ER from nuclear sites. Consequently, it preferentially activates ER from membrane and cytoplasmic sites (ER that is present at these extranuclear locations will be designated mER.).<sup>2,3</sup> As a result of this restriction of its subcellular distribution, EDC activates through mER only a subset of estrogen-regulated responses, the bulk of which are beneficial, without activating reproductive tissues or breast cancer cells that would exacerbate the risk or promotion of cancer.

Some nano-size polymer-drug assemblies employ pH-responsive properties that enable them to effect selective antitumor drug delivery: They remain stable while they accumulate in tumors by the enhanced permeability-retention (EPR) effect, and they then release their active

ingredient because of the low pH in the target zone<sup>18</sup> (extracellular tumor hypoxia, pH ~6.5;<sup>19-21</sup> inflammatory tissue ~5.5;<sup>22</sup> lysosomes, ~4.5).<sup>23</sup> Because it is stably attached to the dendrimer by a stable covalent bond, however, the estrogen in the EDC cannot be released simply by a change in pH. Nevertheless, by affecting the conformation of the PAMAM, changes in pH might influence how accessible the estrogen is to the mER.

PAMAMs, which are becoming increasingly important as vehicles for medical drug delivery,<sup>24-28</sup> are ionizable dendrimeric polyamines; so, one would imagine them to show morphological changes—in size, shape, and internal volume—as a function of pH, reflecting the extent of protonation of their accessible surface/primary amines (pK<sub>a</sub> 7-9) vs. their less basic internal/tertiary amines (pK<sub>a</sub> 3-6).<sup>29-31</sup> These predicted pH-dependent conformational changes of PAMAMs have been studied in considerable detail by molecular simulation,<sup>17,32,33</sup> from which one can surmise that amine-bearing PAMAM dendrimers undergo profound pH-dependent conformation changes of over the physiological range of acidity (pH 4.5-7.4).

Little is known about the stability of these PAMAM conformational states or the functional relationship between these states and the accessibility and activity of bioactive ligands attached to a PAMAM dendrimer surface, all of which could affect the *in vivo* activity, selectivity, and utility of hormone-PAMAM conjugates. In particular, it is important to understand how the *in vivo* activity of a surface-tethered ligand might change over a pH range or even be affected in an irreversible manner by prior exposure to more acidic pH. We are aware of no prior comprehensive study exploring this issue.

Therefore, to probe the behavior of EDC-like PAMAM conjugates in cells and to assist in the design of new agents for future *in vivo* applications, we investigated herein, through photophysical and spectroscopic methods, and by multicolor subcellular-colocalization imaging and cell-based activity assays, the pH-dependent alteration of accessibility and activity of hydrophobic molecules (a fluorophore and two estrogens) covalently attached to the surface of

a G6 PAMAM dendrimer. To mimic the different pH environments that an EDC would encounter physiologically, these samples were preincubated at pH 4.5 (endosome/lysosome environment), 6.5 (hypoxic environment and tumor), 7.0, or 8.5, before being returned to pH 7.4 for cellular bioactivity and localization studies. These studies revealed remarkable pH-dependent alterations in EDC ligand motion and accessibility: Initially, at the alkaline pH used for EDC preparation, the ligand was somewhat constrained but still accessible; then in acidic pH it became highly exposed and dynamic, and finally, after being returned to pH 7, the ligand became—unexpectedly—occluded by the collapsed dendrimeric PAMAM architecture and experienced *full loss of biological activity*. The effect of altered polymer conformations in response to exposure of the EDC to different pH conditions—and pH history—that affect the flexibility and accessibility of pendant ligands on the PAMAM dendrimer surface could have profound consequences for the design and evaluation of other drug-polymer conjugates and their biomedical utility.

## RESULTS

**pH-dependent collisional quenching and time-resolved anisotropy of TMR-conjugated PAMAM G6 dendrimer, a fluorescent surrogate ligand, indicates major alterations in ligand exposure and flexibility.** To facilitate studies of how pH influences PAMAM conformation and ligand accessibility, we used tetramethyl rhodamine (TMR) as a fluorescent model ligand. We attached TMR covalently to the amine-terminated G6 ethylenediamine-core PAMAM dendrimer at the usual pH of 8.5, controlling the surface coverage to be 18~20 TMRs per dendrimer similar to that of our EE<sub>2</sub>-EDC compound (**Figure 2A**).<sup>3,4</sup>

We first explored the surface exposure of the dendrimer-bound TMRs by measuring the collisional fluorescence quenching effect of potassium iodide (KI).<sup>34</sup> The TMR-dendrimer conjugate was titrated with aqueous KI at three different pH's (**Figure 2B**). The quenching effect changed dramatically between pH 4 and 7, with the Stern-Volmer plot slope at pH 4 being 20-fold greater than at pH 7.0; by contrast, the slope declined only three-fold between pH 7-9. This suggests that as the pH was increased from 4 to 7, a marked change in dendrimer conformation occurs, progressively shielding the TMRs from exposure to KI; the conformational changes that occur between pH 7-9, however, result in only a moderate increase in ligand shielding.

This is interesting because the TMR-dendrimer conjugate was prepared at pH 8.5, conditions under which most surface/primary amines and inner/tertiary amines would be deprotonated. With little Coulombic repulsion to oppose it, the hydrophobic effect should force the dendrimer structure to collapse into a tightly compacted conformation, minimizing the volume and aqueous solvent-accessible surface of the more hydrophobic core.<sup>31</sup> Nevertheless, one might expect that the KI quencher would still have good accessibility to most of the TMRs on the dendrimer surface. Consequently, it is not clear why the quenching effect of KI at pH 9 would be so different from that at pH 4. These results led us to reconsider the accessibility—and



potentially the activity—of hormonal ligands attached to the surface of a G6 PAMAM dendrimer as a result of the pH of the environment.

To further characterize ligand conformation and accessibility, we used time-dependent fluorescence anisotropy to explore how the local motion of individual TMRs correlated with the global tumbling of the dendrimer. We adapted a time-correlated single photon counting system<sup>35</sup> to measure total anisotropy and deconvolute the local and global movement of TMRs attached to the dendrimer over pH 2-9 (**Figure 2CD**).

Regardless of pH, the anisotropy decays displayed a bi-exponential pattern (**Figure 2C**): The fast-tumbling population (0.5–1.3 ns) was highest at pH 2, where it actually exceeded the slow-tumbling population (8.3–14.3 ns) (**Figure 2D and Supplementary Table S1**). At acidic pH, the PAMAM dendrimer would be highly protonated and thus because of Coulombic repulsion should favor a loose, extended conformation, providing room and flexibility for the TMRs at the ends of the dendrimer arms to tumble freely. The fraction of fast-moving species showed a progressive decrease with increasing pH until pH 7; beyond this, this fraction did not change. Thus, in terms of TMR access to KI quenching and fast motion, pH 7 seems to be an important break point that divides looser, more flexible structural conformations of amine-terminated G6 PAMAM dendrimer (below 7) from tighter, more rigid ones (above 7). These pH-dependent alterations of PAMAM dendrimer conformations could alter the activity of bioactive ligands attached to this pH-responsive dendrimer.

**Dynamic <sup>1</sup>H NMR studies of EDC highlights pH-dependent changes in ligand flexibility and a transition to a ligand-buried state.** To explore how pH determines whether the bioactive estrogenic ligands (EE<sub>2</sub> and diphenolic acid [DPA]) attached to the EDC surface are either confined or accessible to the membrane ER (mER), we prepared an EE<sub>2</sub>-EDC sample with 20 EE<sub>2</sub> molecules per dendrimer as usual at pH 8.5.<sup>4</sup> We then determined for the three

aromatic A-ring protons of  $EE_2$  on the surface of EDC compound, the rotational correlation times ( $\tau_c$ ) by measuring T2 (spin-spin relaxation time) and T1 (spin-lattice relation time) after EDC exposure to different pH's in  $D_2O$  (**Figure 3**, for more detailed information see **Supplementary Figure S2** and **Tables S2**). In each panel, the numbers indicate T2 values as line width at half-height (in black), and rotational correlation times ( $\tau_c$ ) in nanoseconds (in red).<sup>36</sup> The measured rotational correlation time for each peak, at different pHs, reflects an ensemble movement averaged over the 20  $EE_2$  molecules on the surface of G6 PAMAM dendrimer.

When the pH was lowered from 8.5 to 4.5,  $\tau_c$  values were 10-15% faster than at the original pH 8.5. The  $\tau_c$  values became slower when the pH was raised back to 6.5, at which point they are similar to the original values at pH 8.5. Remarkably, when the EDC was taken through the full pH cycle, from the original pH 8.5 to pH 4.5 and then all the way back to pH 8.5,  $\tau_c$  values became even 25-35% slower than they were originally at pH 8.5. This suggests that after the pH cycle, a larger portion of  $EE_2$  ligands becomes confined within the dendrimer framework, thereby experiencing the more greatly retarded ensemble motion.

The associated T2 values, which are directly proportional to the line broadening experienced by a small molecule in the vicinity of a polymeric environment, show a similar trend with the pH cycle of the EDC: They become narrower (longer T2) at acidic pH, when returned to pH 6.5, as broad as they were *originally* at pH 8.5, and then finally even broader when raised back to pH 8.5 (shorter T2). This behavior is again consistent with the motion of the surface ligands becoming more constrained by being caught within the interior of the polymer after the cycle through acidic pH.

Both fluorescence anisotropy and dynamic NMR experiments indicate that pH-dependent alterations of the dendrimer framework influence in a similar way the flexibility of pendant ligands, either TMR or  $EE_2$ , on the surface of the G6 PAMAM dendrimer. The key observation made from measuring  $\tau_c$  and T2 values through a pH cycle is that *after cycling the EDC from pH*

8.5 to pH 4.5 and then back to pH 8.5, the  $EE_2$  ligands, originally on the PAMAM surface and accessible, appear to have become more buried within the PAMAM skeleton than before. This change could have a significant effect on ligand activity, and it suggests that the EDC as initially prepared at pH 8.5 is in an active but metastable conformational state that, after being cycled to pH 4.5 and then back to 8.5, undergoes further conformational changes that bury the ligand and render the EDC inactive.

**Gene expression patterns for EDC and DPA-dendrimer are affected by prior exposure to different pH.** These observations prompted us to investigate the biological activity of EDC in a cellular context as a function of its “pH history”. An EDC sample, prepared at pH 8.5, was split into four aliquots, which were either maintained at pH 8.5 or adjusted to pH 7.0, 6.5, or 4.5. After a period of time (1 hr to 1 day), a small portion of each sample was then returned to pH 7.4 by being diluted ~10,000 fold into pH 7.4 tissue culture media containing human breast cancer (MCF-7) cells; the level of expression of five representative genes was then determined for each of the EDC preparations having differing “pH histories” (**Figure 4**).

Three of these genes (CISH, PMAIP1, and LRRC54; **Figure 4** top panel) are known to be driven by the extra-nuclear action of the membrane estrogen receptor (mER, termed “non-genomic” activity) and are effectively stimulated by EDC prepared under the conventional, high pH protocol and by estradiol ( $E_2$ ), whereas two of these genes (PgR and pS2; **Figure 4** bottom panels) are known to require direct nuclear-initiated ER action (termed “genomic”) and are stimulated by  $E_2$  but not by EDC.<sup>3,8</sup> MCF-7 cells were treated with each  $EE_2$ -EDC sample (10 nM  $EE_2$  equivalent concentration) at pH 7.4 for 4 hours, and the level of gene expression was determined by qPCR analysis.

As expected, none of the EDC samples stimulated the genomic genes (**Figure 4** bottom).<sup>8</sup> Notably, while the EDC originating from the pH 7.0 and pH 8.5 samples stimulated the non-

genomic genes (**Figure 4** top) effectively, the EDC samples that had been exposed to pH 4.5 and 6.5 (but like the others, moved back to pH 7.4 prior to the assay) had essentially no effect on non-genomic gene expression, giving the same response as vehicle or control (underivatized) G6 PAMAM. (The loss of EDC activity on the non-genomic genes is not due to loss of ligand by cycling to acidic pH; no loss of ligand was observed in the dynamic NMR studies or by MS analysis of EDC before and after the pH cycle; **Supplementary Figure S6**.) The more hydrophilic DPA-DC, which was studied to evaluate the generality of this phenomenon, gave very similar results, activating non-genomic genes if kept at high pH, but not if it was cycled through low pH and back prior to cellular assays (**Supplementary Figure S7**).

Notably, the pH 7 cutoff in EDC-stimulated expression of the non-genomic genes nicely matches the pH 7 cutoffs found in the fluorescence quenching and anisotropy experiments (**Figures 2BCD**). Furthermore, our findings that the pattern of gene expression depends on the pH history on an EDC or DPA-dendrimer preparation are consistent with the results of the NMR rotational correlation time experiments, through which we found that cycling EDC through acidic pH caused ligands to transition from a higher-motion, surface-exposed state to a lower-motion, buried or occluded state.

**Cellular imaging provides further evidence for the effect of pH history on EDC cellular activity and colocalization.** To further explore the impact of pH history on the biological function of EDC and DPA-DC, we monitored activation of the MAPK cascade, a well-recognized action of estrogens through mER,<sup>3,8</sup> and we determined the colocalization of ER $\alpha$  with activated pMAPK1/2 using fluorescence microscopy. Cells treated with Cy5-EDC that had been stored at pH 8.5 (but examined at pH 7.4) showed intense signals from ER $\alpha$  (yellow, largely nuclear) and pMAPK1/2 (green, largely cytoplasmic). Because only 5-10% of ER $\alpha$  resides close to the cell membrane,<sup>37</sup> the Cy5-EDC signal (red) appeared as punctate peri-membrane spots (as seen

before<sup>2,3</sup>), and these were colocalized with a subfraction of both ER $\alpha$  and pMAPK (**Figure 5A**).

By contrast, the EDC samples that had been exposed to pH 6.5 caused minimal activation of pMAPK1/2 and showed minimal colocalization with ER $\alpha$  and pMAPK1/2 (**Figure 5B**).

Control experiments in the presence and absence of Cy5-labeled PAMAM G6 dendrimer without any ligand (**Figure 5C**) showed clearly that the MAPK activation and colocalization observed in **Figure 5A** are ligand-dependent phenomena. In addition, colocalization of Cy5-DPA-DC, DPA being a ligand structurally similar to TMR (**Supplementary Figure S3**), showed the same behavior as EDC: Cy5-DPA-DC maintained at pH 8.5 colocalized with ER $\alpha$  and pMAPK1/2, but did not once exposed to pH 6.5 (**Supplementary Figure S8**).

Proximity ligation assays<sup>38</sup> were used to examine with higher spatial sensitivity whether the co-localized peri-membrane speckles seen in **Fig. 5A** and **Supplementary Fig. S8** represent real interaction among ER $\alpha$ , pMAPK, and EDC (or DPA-DC) (**Figure 6**). The strong speckled signals (bottom correlation histogram of left panels), attributed to the ligation product of ER $\alpha$  interacting with pMAPK1/2, were exactly congruent with the signal for EDC (middle correlation histogram; overlay at top) outside the nucleus, providing further evidence that the multiple ligands on the dendrimer surface are able to activate ER $\alpha$  outside the nucleus, promoting its interaction with pMAPK1/2 to initiate a kinase cascade.

Overall then, the striking correspondence relating kinase activation, EDC/ER $\alpha$ /pMAPK1/2 colocalization, and patterns of gene expression for the EDC samples provide further evidence that the surface ligands retain good activity in EDC samples not exposed to acidic conditions, but that an excursion through acidic pH and return to physiological conditions causes the surface ligands to become confined within the interior of the PAMAM dendrimer (supported by the dynamic NMR studies), resulting in loss of their biological activity.

## DISCUSSION

We have demonstrated, using spectroscopic analyses, cellular bioactivity assays, and subcellular microscopic imaging, that pH cycling of EDC—from normal physiological to acidic and back again—causes the ligand to become buried within the hydrophobic core of the dendrimer, occluding it from interaction with mER and thereby eliminating its biological activity. While pH induced aggregation of the EDC rather than ligand occlusion might, in principle, account for all or some of this loss of biological activity, using dynamic light scattering measurements (DLS), we found essentially no change in the hydrodynamic diameter of the EDC as a result of prior exposure to acidic pH (*Figure S10*). Hence, ligand occlusion rather than aggregation appears to be the most likely mechanism to account for the loss of EDC biological activity from cycling to low pH conditions.

A schematic representation of the three states of the EDC at different pH's and their potential interactions with a membrane bilayer and mER, developed by molecular dynamics simulations and drawn to scale, is given in **Figure 7**. At the pH of EDC synthesis (8.5), the largely deprotonated G6 PAMAM is compact and condensed, yet its surface amines are able to react efficiently with the derivatizing reagent for EE<sub>2</sub> or other ligands, producing hormone-dendrimer conjugates having ligands that are external (right, blue PAMAM, grey/red EE<sub>2</sub>), though not very mobile (little fast motion in the anisotropy experiment) nor well exposed to quenching by KI. This state can be termed “Surface Compact”, and it appears to be the initial state of the conjugates after preparation and also when they are moved only to pH 7.4, the condition of the cell assays for all of the EDC. Upon interaction with the cell membrane, the hydrophobic ligands on the surface-compact form of the EDC are sufficiently exposed that they can be accessed by the cytoplasmic or membrane fraction of estrogen receptor (mER, green), and interaction that results in the activation of protein kinase cascades leading to expression of non-genomic genes; this interaction might involve or be followed by endocytosis.

By contrast, when the surface-compact form of the EDC is exposed to acidic conditions (pH 6.5, but especially pH 4.5), it undergoes a pronounced conformational change to an “Expanded” form, in which Coulombic repulsion between the highly protonated amines expands the dendrimer volume, extending the arms bearing the ligands (*middle*). In this state, the ligands undergo rapid tumbling and are very accessible to KI quenching.

When the expanded form of the EDC is returned to pH 7.4, by being diluted into the cell assay medium at this pH, it does not return to the original surface-compact form. Rather, we propose that when the dendrimer is in the expanded state, the lipophilic EE<sub>2</sub> ligands have, for the first time, an opportunity to explore the more hydrophobic interior of the PAMAM dendrimer. With rising pH, during the process of dendrimer recondensation, the lipophilic ligands become trapped in the dendrimer interior, forming what can be termed an “Occluded” state of the EDC (*left*). In this occluded state, the sequestered ligands (*left*, gray-red ligands less visible) are not able to access the mER; thus, this form of the EDC shows little cellular activity. With lipophilic ligands like EE<sub>2</sub>, it is likely that the occluded state is more stable than the surface-compact state, because the lipophilic ligand, given the opportunity, prefers to reside in the more hydrophobic core of the PAMAM than on the more polar dendrimer surface.

This three-state model for the conformation and activity of EDC-like drug-PAMAM dendrimer conjugates suggests that such molecules might be engineered to have other unusual forms of selectivity. Nano-sized PAMAM covalent conjugates of cytotoxic drugs could first be induced to adopt the occluded state by cycling through acidic pH, and thus would have low activity on normal cells. Dendrimers that become trapped in tumors by the enhanced permeability and retention (EPR) effect,<sup>39,40</sup> however, would adopt the extended conformation in response to the local acidic environment of the tumor or in acidified vesicles after endocytosis, exposing tumor cells selectively to the cytotoxic effect of the drug. Other approaches to regulate extracellular vs. intracellular activity of drug-PAMAM dendrimer conjugates can be envisioned.

## CONCLUSIONS

In summary, we have elucidated the behavior of ligands tethered to the surface of amine-bearing G6 PAMAM dendrimers using TMR as a fluorescent ligand surrogate for the bioactive hormone, ethynyl estradiol ( $EE_2$ ). This enabled us to evaluate ligand exposure by fluorescence quenching and ligand motion by time-domain fluorescence polarization. In addition, measurement of rotational correlation times ( $\tau_c$ ) and spin-spin relaxation times ( $T_2$ ) of EDC itself provided information on global changes in the population of surface-bound hormone, indicating whether they are accessible, extended, or occluded as a function of pH or their pH history. The greater mobility and exposure of the ligand at acidic pH, together with the high activity of the EDC prepared and maintained at alkaline pH vs. the low activity of EDCs that were cycled through low pH, are consistent with a three-state model for EDC conformation in which selective activity in stimulating non-genomic gene responses in target cells is mediated only by the ligand-accessible, surface-compact, active form of EDC. Notably, this form is metastable and can be induced to relax, resulting in an occluded, inactive state, by cycling through acidic pH. This model should provide a useful guide for the design and evaluation of other drug-PAMAM dendrimer conjugates.



## Experimental

### Materials and Methods

<sup>1</sup>H NMR and <sup>13</sup>C NMR spectra were recorded on a Varian Inova-500 with D<sub>2</sub>O. MALDI-TOF (Matrix Assisted Laser Desorption Ionization-Time Of Flight) mass analysis (2,5-dihydroxybenzoic acid, DHB, as a matrix) and electrospray ionization mass spectra were obtained using Voyager-DE<sup>TM</sup> STR and a Q-TOF Ultima API (Waters Co. Ltd), respectively. Fluorescence experiments used a Spex Fluorolog II (model IIIc) cuvette-based fluorometer with Data Max 2.2 software (Spex Industries, Edison, NJ). All data were analysed with Origin 7.5 (OriginLab Co., Massachusetts, USA) and All data were analyzed using Prism 5.0 (GraphPad Software, San Diego, CA). Compounds and materials were obtained from the sources indicated: Diphenolic acid (TCI America co. Montgomeryville, PA), ethylene diamine core amine-terminated generation 6 PAMAM dendrimer (Aldrich Inc. St. Louis, MO), TMR-NHS ester (Berry & Associates, Inc. Dexter, MI).

**TMR-conjugated PAMAM dendrimer.** To the solution of ethylenediamine-core G6 PAMAM dendrimer (86 nmol, 5 mg, 100 mg 5% in 400  $\mu$ L MeOH) was added TMR-NHS ester (2.06  $\mu$ mol, 1.09 mg in 50  $\mu$ L DMF) (Berry & Associates, Inc. Dexter, MI) in MeOH and continuously stirred for 1 hr. The reaction mixture was transferred into 3 mL 30K cutoff Amicon filter (Millipore Inc.) and diluted with water (2 mL) before being centrifuged multiple times (466 x g) to eliminate free ligand. The pellet liquid was transferred into a small vial and dried to give a film of a viscous liquid, which was kept under nitrogen and used to make a stock solution (~15 mM TMR or DPA equivalent) in methanol. The pH of a small aliquot was adjusted with 5N HCl and 0.1N HCl, 5N NaOH, 0.1N NaOH, by microtitration, based on the assumption that 510 total inner tertiary and outer primary amines remain in the PAMAM G6 dendrimer after ligand conjugation. All data were analyzed with Origin 7.5 (OriginLab Co., Massachusetts, USA).

**KI quenching experiments.** Potassium iodide (KI) quenching experiments used a Spex Fluorolog II (model IIIc) cuvette-based fluorometer with Data Max 2.2 software (Spex Industries, Edison, NJ). Excitation was at 541 nm and emission at 580 nm. Aliquots of the TMR-dendrimer conjugate at 100 nM TMR equivalents in MeOH were adjusted to pH 4, 7 and 9 and then titrated with 0-150 mM KI (in 10 mM Na<sub>2</sub>S<sub>2</sub>O<sub>3</sub>).

**Time-resolved fluorescence anisotropy measurements.** Fluorescence anisotropy was measured with a home-built time-correlated single photon counting system. Two-photon excitation of the fluorescent probe molecules was induced using a femtosecond Ti:Sapphire laser (Tsunami, Spectra-physics) with 100 fs pulse width. The repetition rate was 80 MHz, and the wavelength was 800 nm. Fluorescence was excited and collected by the same objective lens (LD-Neofluar, NA=0.7, Carl Zeiss) at confocal geometry. The fluorescence signal was split into two perpendicular polarizations and monitored simultaneously by two fast avalanche photodiodes (id100-50, IDQ). Details of the experimental setup are described elsewhere<sup>35</sup>.

**Rotational correlation time measurement by NMR.** ~20 EE<sub>2</sub>-conjugated EDC (32 mg) was dissolved into 0.65 mL D<sub>2</sub>O, followed by adjusting pH with 35 wt% 0.1 N DCl in D<sub>2</sub>O and 40 wt% 0.1N NaOD in D<sub>2</sub>O using a micro syringe, based on the total number of amines on the dendrimer. (pH values were confirmed by pH-indicator paper; non-bleeding pH 5.0 to 10.0, MColorpHast<sup>TM</sup>, EMD Millipore) To minimize magnetic field inhomogeneity, spectra were obtained from the same NMR tube. T1 and T2 values were determined on a Varian Unity-500 narrow bore NMR spectrometer using a Hahn echo decay experiment and an inversion-recovery method, respectively, using internally installed software. Correlation times were determined by the polynomial function  $\tau_c(\text{ns}) = a_0 + a_1(R_2/R_1) + a_2(R_2/R_1)^2 + a_3(R_2/R_1)^3 + a_4(R_2/R_1)^4$ , where  $R_1/R_2 = T_2/T_1$ , and the values for  $a_0$ ,  $a_1$ ,  $a_2$ ,  $a_3$ , and  $a_4$  were taken from the literature<sup>36</sup>.

**Cell culture, RNA extraction, and real-time PCR analysis of gene expression regulation.**

MCF-7 human breast cancer cells, which contain high levels of ER $\alpha$ , were maintained in culture as previously described<sup>41</sup>. At 6d before E<sub>2</sub> treatment, cells were switched to phenol red-free media containing charcoal-dextran-treated calf serum. Medium was changed on d2 and d4 of culture, and cells were then treated with 10 nM E<sub>2</sub> or 10 nM E<sub>2</sub> equivalent EDC for 4 h. After cell treatments, total RNA was isolated, reverse-transcribed, and analyzed by real-time PCR, as described previously<sup>41</sup>. Primers for the estrogen-regulated genes HSPB8, CISH, PMAIP1, LRRC54, PgR, and pS2 have been described previously<sup>3,8</sup>.

**Immunofluorescence microscopy for colocalization studies.** MCF-7 cells were treated for 15 min with Cy5-labeled EDC, which had been stored at the indicated pH, and Cy5-Empty dendrimer. Cells were then washed in PBS and fixed on glass coverslips in 4% paraformaldehyde for 30 min and washed two times for 5 min in PBS. After incubation in acetone for 5 min, another PBS wash was performed and then cells were incubated with ER $\alpha$  antibody (F10, Santacruz Biotech.) and pMAPK1/2 antibody (9101, Cell Signaling) overnight. The cells were then incubated with goat anti mouse Alexa-568 and goat anti-rabbit Alexa-488 secondary antibodies. These slides were mounted and stained using Prolong Gold antifade with 4,6-diamidino-2-phenylindole (DAPI, Molecular Probes) to identify the nuclei. Samples were observed with a LSM 710 confocal microscope, and fluorescence images (20 optical sections per cell) were collected and overlaid using ZEN 2011 software.

**Proximity ligation assay (PLA).** The proximity ligation assay (PLA assay) was performed using the Duolink In Situ kit (Olink Bioscience) according to the manufacturer's instructions. Briefly, cells were treated and prepared similar to immunofluorescence methods. Overnight incubation with primary antibodies was followed by hybridization with two PLA probes at 37 °C for 1 h, and then by ligation for 15 min and amplification for 90 min at 37 °C. A cover slip was mounted on the slide after PLA to acquire and analyze images as above.

## Acknowledgements

We are grateful for support of this research through grants from the U.S. Department of Energy, Division of Materials Science (fluorescence anisotropy measurements supported by DEFG02-02ER46019 to S.G.), the Institute for Basic Science, Project Code IBS-R020-D1 to SG) and the U.S. National Institutes of Health (PHS 5R37DK015556 to J.A.K.). NMR spectra were obtained in the Varian Oxford Instrument Center for Excellence in NMR Laboratory at University of Illinois.

**Supporting Information Available** Molecular modeling, full structure of EDC, proton NMR for EDC at different pH, synthesis of DPA-dendrimer conjugate, gene expression data and colocalization microscopic picture for DPA-dendrimer, and an analysis of T1 and T2. This material is available free of charge via the Internet at <http://pubs.acs.org>.

## References

- (1) Maximov, P. Y.; Lee, T. M.; Jordan, V. C. *Curr Clin Pharmacol* **2013**, *8*, 135.
- (2) Chambliss, K. L.; Wu, Q.; Oltmann, S.; Konaniah, E. S.; Umetani, M.; Korach, K. S.; Thomas, G. D.; Mineo, C.; Yuhanna, I. S.; Kim, S. H.; Madak-Erdogan, Z.; Maggi, A.; Dineen, S. P.; Roland, C. L.; Hui, D. Y.; Brekken, R. A.; Katzenellenbogen, J. A.; Katzenellenbogen, B. S.; Shaul, P. W. *J. Clin. Invest.* **2010**, *120*, 2319.
- (3) Harrington, W. R.; Kim, S. H.; Funk, C. C.; Madak-Erdogan, Z.; Schiff, R.; Katzenellenbogen, J. A.; Katzenellenbogen, B. S. *Mol. Endocrinol.* **2006**, *20*, 491.
- (4) Kim, S. H.; Katzenellenbogen, J. A. *Angew. Chem. Int. Ed. Engl.* **2006**, *45*, 7243.
- (5) Chakravarty, D.; Nair, S. S.; Santhamma, B.; Nair, B. C.; Wang, L.; Bandyopadhyay, A.; Agyin, J. K.; Brann, D.; Sun, L.-Z.; Yeh, I.-T.; Lee, F. Y.; Tekmal, R. R.; Kumar, R.; Vadlamudi, R. K. *Cancer Res.* **2010**, *70*, 4092.
- (6) Fan, P.; Griffith, O. L.; Agboke, F. A.; Anur, P.; Zou, X.; McDaniel, R. E.; Creswell, K.; Kim, S. H.; Katzenellenbogen, J. A.; Gray, J. W.; Jordan, V. C. *Cancer Res.* **2013**, *73*, 4510.
- (7) Kousteni, S.; Almeida, M.; Han, L.; Bellido, T.; Jilka, R. L.; Manolagas, S. C. *Mol. Cell. Biol.* **2007**, *27*, 1516.
- (8) Madak-Erdogan, Z.; Kieser, K. J.; Kim, S. H.; Komm, B.; Katzenellenbogen, J. A.; Katzenellenbogen, B. S. *Mol. Endocrinol.* **2008**, *22*, 2116.
- (9) Adlanmerini, M.; Solinhac, R.; Abot, A.; Fabre, A.; Raymond-Letron, I.; Guihot, A. L.; Boudou, F.; Sautier, L.; Vessieres, E.; Kim, S. H.; Liere, P.; Fontaine, C.; Krust, A.; Chambon, P.; Katzenellenbogen, J. A.; Gourdy, P.; Shaul, P. W.; Henrion, D.; Arnal, J. F.; Lenfant, F. *Proc. Natl. Acad. Sci. U. S. A.* **2014**, *111*, E283.
- (10) Alyea, R. A.; Laurence, S. E.; Kim, S. H.; Katzenellenbogen, B. S.; Katzenellenbogen, J. A.; Watson, C. S. *J. Neurochem.* **2008**, *106*, 1525.
- (11) Yang, L.-c.; Zhang, Q.-G.; Zhou, C.-f.; Yang, F.; Zhang, Y.-d.; Wang, R.-m.; Brann, D. W. *PLoS ONE* **2010**, *5*, e9851.
- (12) Tiano, J. P.; Delghingaro-Augusto, V.; Le May, C.; Liu, S.; Kaw, M. K.; Khuder, S. S.; Latour, M. G.; Bhatt, S. A.; Korach, K. S.; Najjar, S. M.; Prentki, M.; Mauvais-Jarvis, F. *The Journal of Clinical Investigation* **2011**, *121*, 3331.
- (13) Tiano, J. P.; Mauvais-Jarvis, F. *Endocrinology* **2012**, *153*, 2997.
- (14) Wong, W. P. S.; Tiano, J. P.; Liu, S.; Hewitt, S. C.; Le May, C.; Dalle, S.; Katzenellenbogen, J. A.; Katzenellenbogen, B. S.; Korach, K. S.; Mauvais-Jarvis, F. *Proceedings of the National Academy of Sciences* **2010**, *107*, 13057.
- (15) Bartell, S. M.; Han, L.; Kim, H.-n.; Kim, S. H.; Katzenellenbogen, J. A.; Katzenellenbogen, B. S.; Chambliss, K. L.; Shaul, P. W.; Roberson, P. K.; Weinstein, R. S.; Jilka, R. L.; Almeida, M.; Manolagas, S. C. *Mol. Endocrinol.* **2013**, *27*, 649.
- (16) Li, Z.; Chen, K.; Jiao, X.; Wang, C.; Willmarth, N. E.; Casimiro, M. C.; Li, W.; Ju, X.; Kim, S. H.; Lisanti, M. P.; Katzenellenbogen, J. A.; Pestell, R. G. *Cancer Res.* **2014**, *74*, 3959.
- (17) Liu, Y.; Bryantsev, V. S.; Diallo, M. S.; Goddard Iii, W. A. *J. Am. Chem. Soc.* **2009**, *131*, 2798.
- (18) Nowag, S.; Haag, R. *Angewandte Chemie International Edition* **2014**, *53*, 49.
- (19) Chiche, J.; Ilc, K.; Laferrière, J.; Trottier, E.; Dayan, F.; Mazure, N. M.; Brahimi-Horn, M. C.; Pouyssegur, J. *Cancer Res.* **2009**, *69*, 358.
- (20) Frechet, J.; Schuerch, C. *J. Am. Chem. Soc.* **1969**, *91*.
- (21) Švastová, E.; Hulíková, A.; Rafajová, M.; Zatořovičová, M.; Gibadulinová, A.; Casini, A.; Cecchi, A.; Scozzafava, A.; Supuran, C. T.; Pastorek, J. r.; Pastoreková, S. *FEBS Lett.* **2004**, *577*, 439.

- (22) Steen, K.; Steen, A.; Reeh, P. *The Journal of Neuroscience* **1995**, *15*, 3982.
- (23) Mindell, J. A. *Annu. Rev. Physiol.* **2012**, *74*, 69.
- (24) Esfand, R.; Tomalia, D. A. *Drug Discovery Today* **2001**, *6*, 427.
- (25) Kitchens, K. M.; Ghandehari, H.; Villiers, M. M.; Aramwit, P.; Kwon, G. S., Eds.; Springer New York: 2009; Vol. X, p 423.
- (26) Yellepeddi, V. K.; Kumar, A.; Palakurthi, S. *Anticancer Res.* **2009**, *29*, 2933.
- (27) Kannan, R. M.; Nance, E.; Kannan, S.; Tomalia, D. A. *J. Intern. Med.* **2014**, *276*, 579.
- (28) Tomalia, D. A.; Christensen, J. B.; Boas, U. *Dendrimers, dendrons, and dendritic polymers: discovery, applications, and the future*; Cambridge University Press, 2012.
- (29) Kleinman, M. H.; Flory, J. H.; Tomalia, D. A.; Turro, N. J. *The Journal of Physical Chemistry B* **2000**, *104*, 11472.
- (30) Chen, W.; Tomalia, D. A.; Thomas, J. L. *Macromolecules* **2000**, *33*, 9169.
- (31) Tomalia, D. A.; Baker, H.; Dewald, J.; Hall, M.; Kallos, G.; Martin, S.; Roeck, J.; Ryder, J.; Smith, P. *Polymer Journal* **1985**, *17*, 117.
- (32) Tanis, I.; Karatasos, K. *Phys. Chem. Chem. Phys.* **2009**, *11*, 10017.
- (33) Lee, I.; Athey, B. D.; Wetzel, A. W.; Meixner, W.; Baker, J. R. *Macromolecules* **2002**, *35*, 4510.
- (34) Jameson, D. M.; Gratton, E.; Eccleston, J. F. *Biochemistry* **1987**, *26*, 3894.
- (35) Jeon, S.; Bae, S. C.; Granick, S. *Macromolecules* **2001**, *34*, 8401.
- (36) Carper, W. R.; Keller, C. E. *The Journal of Physical Chemistry A* **1997**, *101*, 3246.
- (37) Levin, E. R. *Mol. Endocrinol.* **2011**, *25*, 377.
- (38) Soderberg, O.; Gullberg, M.; Jarvius, M.; Ridderstrale, K.; Leuchowius, K. J.; Jarvius, J.; Wester, K.; Hydbring, P.; Bahram, F.; Larsson, L. G.; Landegren, U. *Nat. Methods* **2006**, *3*, 995.
- (39) Maeda, H.; Wu, J.; Sawa, T.; Matsumura, Y.; Hori, K. *J. Controlled Release* **2000**, *65*, 271.
- (40) Haag, R.; Kratz, F. *Angewandte Chemie International Edition* **2006**, *45*, 1198.
- (41) Frasor, J.; Danes, J. M.; Komm, B.; Chang, K. C. N.; Lyttle, C. R.; Katzenellenbogen, B. S. *Endocrinology* **2003**, *144*, 4562.

1  
2  
3  
4  
5  
6  
7  
8  
9  
10  
11  
12  
13  
14  
15  
16  
17  
18  
19  
20  
21  
22  
23  
24  
25  
26  
27  
28  
29  
30  
31  
32  
33  
34  
35  
36  
37  
38  
39  
40  
41  
42  
43  
44  
45  
46  
47  
48  
49  
50  
51  
52  
53  
54  
55  
56  
57  
58  
59  
60

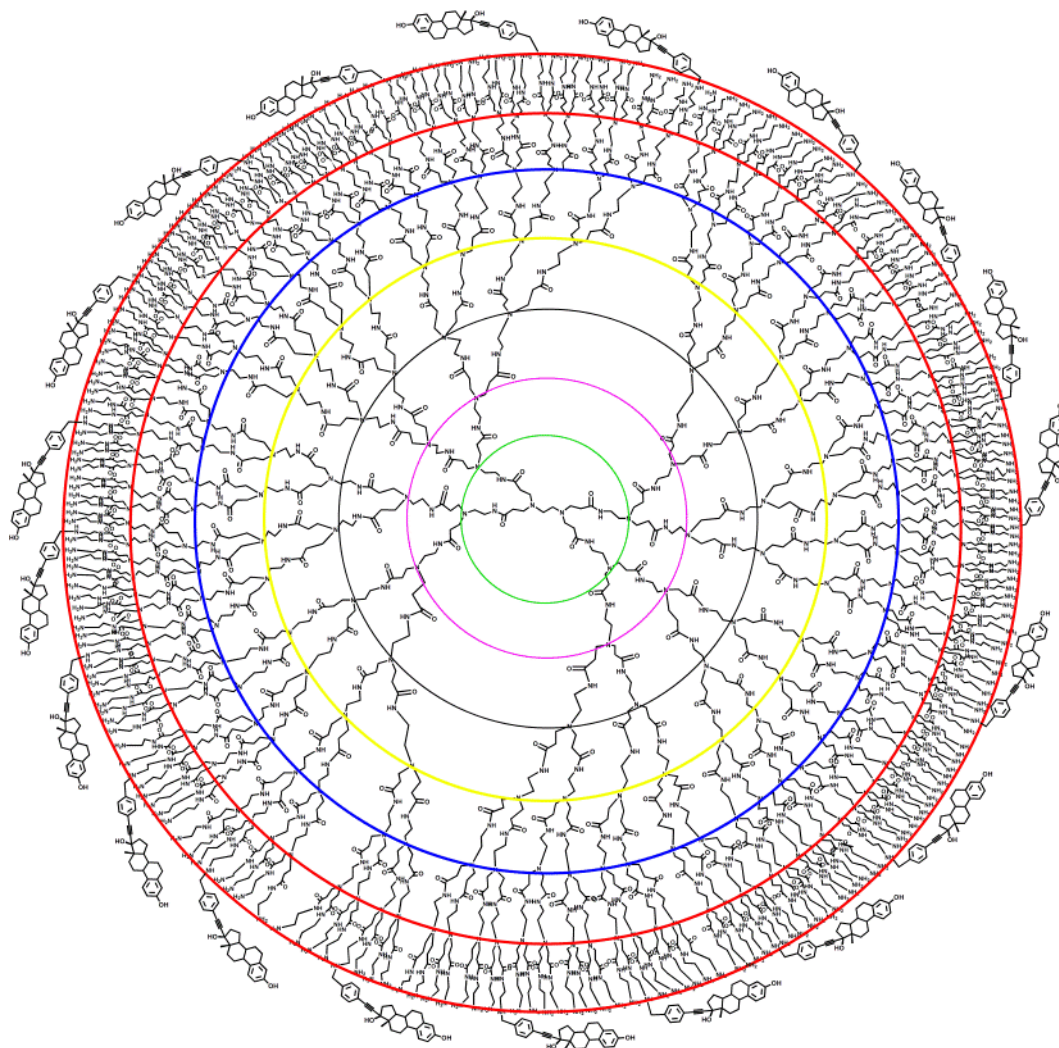


**Figure 1. Full structure of twenty 17 $\alpha$ -(4-phenylmethylene)ethynylestradiol conjugated PAMAM G6 (EDC)**



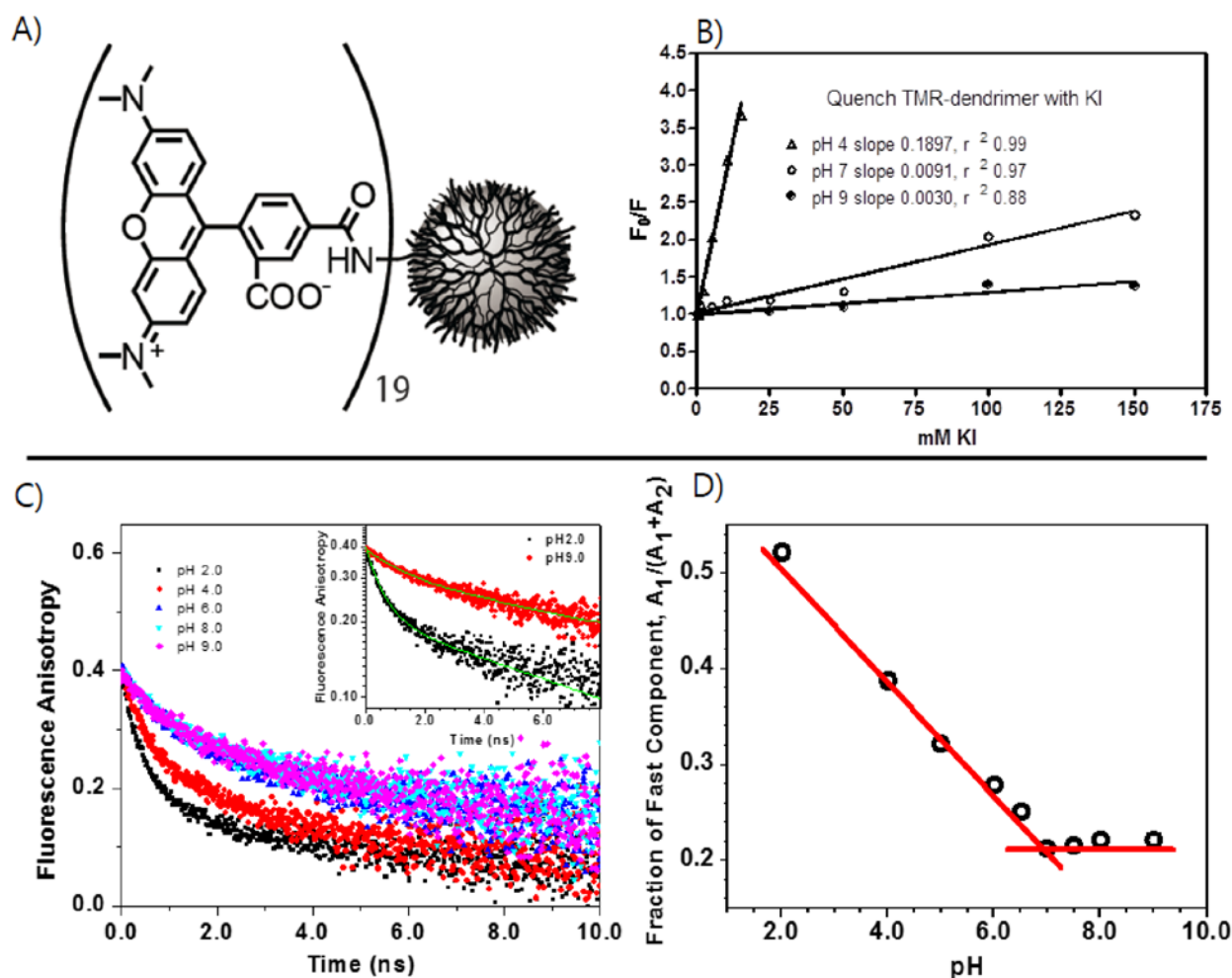


**Figure 2. Collisional quenching by potassium iodide (KI) and time-resolved anisotropy measurement by time-correlated single-photon counting. A, B.** TMR-conjugated G6 PAMAM dendrimer. Fluorescence from a (TMR)<sub>19</sub>-PAMAM dendrimer (100 nM TMR equivalent concentration) in MeOH was quenched by increasing concentrations of KI (0-150 mM). The emission intensity data were analyzed according to the Stern-Volmer equation,  $F_0/F = 1 + K_{sv}[Q]$ , before and after adding KI, at pH 4, 7, and 9. (Ex. 541 nm, Em. 580 nm); **C.** Representative time-resolved anisotropy measurements of TMR conjugated-G6 PAMAM dendrimer over the pH range 2-9. The inset shows the measurements at pH 2 and 9 fitted to a bi-exponential function,  $y = A_1 \cdot \exp(-t/\tau_1) + A_2 \cdot \exp(-t/\tau_2) + y_0$ , where  $\tau_1$  and  $\tau_2$ , the fast and slow

fluorescence decay times in nanoseconds, are considered to correspond to the local tumbling of individual TMR molecules and global tumbling of the whole PAMAM dendrimer, with  $A_1$  and  $A_2$  being the respective populations of these states. **D.** The ratio obtained from the formula  $A_1/(A_1+A_2)$  was plotted versus pH, where  $A_1$  and  $A_2$  designate the populations of the fast and slow motions of TMR, respectively. (The detailed structure of the TMR dendrimer conjugate and its preparation and characterization are given in supplementary information **Figures S3-5.**)

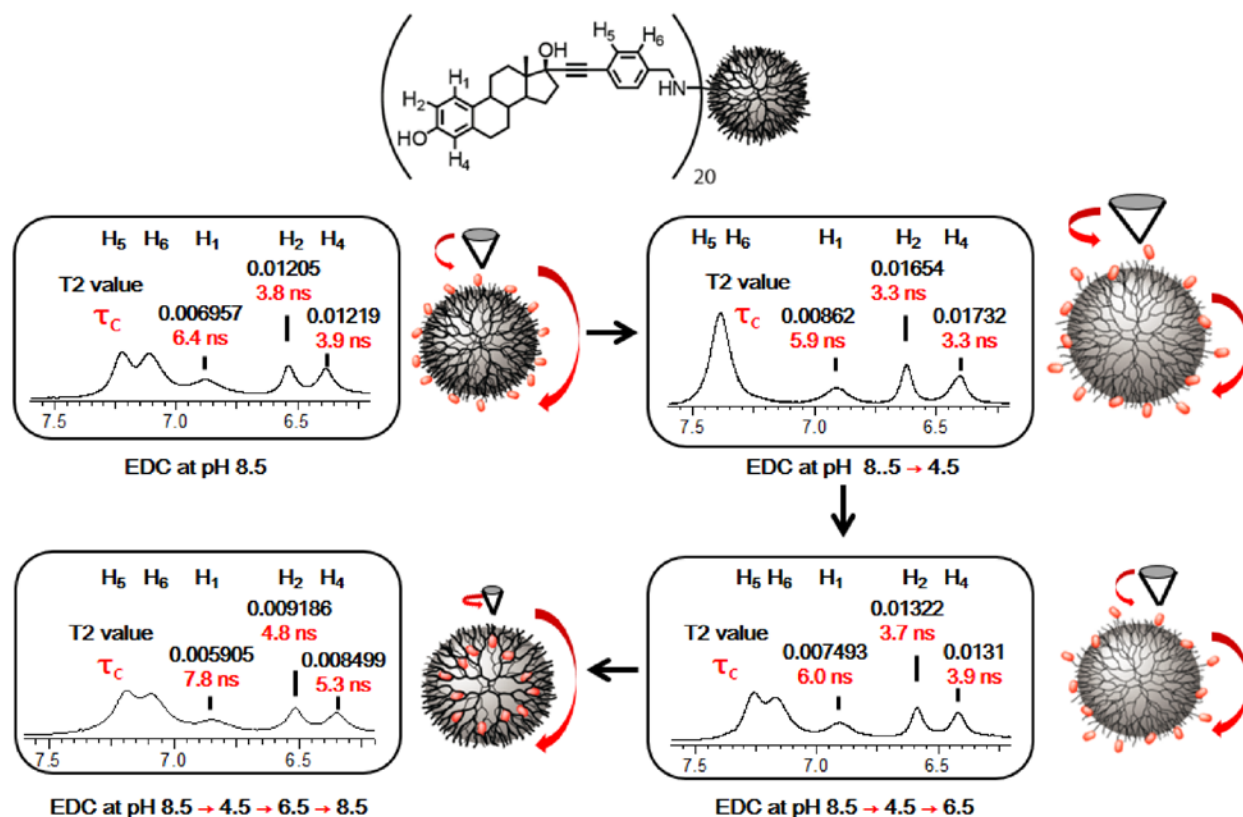


**Figure 3. Rotational correlation time ( $\tau_c$ ) and T2 (spin-spin relaxation time)**

**measurements.** These describe the influence of ensemble movement and line broadening on the A ring of the estradiol moiety driven by small molecule-polymer interactions according to pH. Line width at half-height =  $1/\pi T_2$ , as well as T2 values and  $\tau_c$  (ns) are given at the top of each peak in black and red, respectively. The size of the small red arrow and cone at the top of dendrimer cartoon indicates the degree of local tumbling; the size of the large red arrow at the right side of cartoon indicates the degree of global tumbling. The correlation times were determined by the polynomial function,  $\tau_c(\text{ns}) = a_0 + a_1(R_2/R_1) + a_2(R_2/R_1)^2 + a_3(R_2/R_1)^3 + a_4(R_2/R_1)^4$ , where  $R_1/R_2 = T_2/T_1$  and the values for  $a_0$ ,  $a_1$ ,  $a_2$ ,  $a_3$ , and  $a_4$  were taken from the literature<sup>36</sup>.

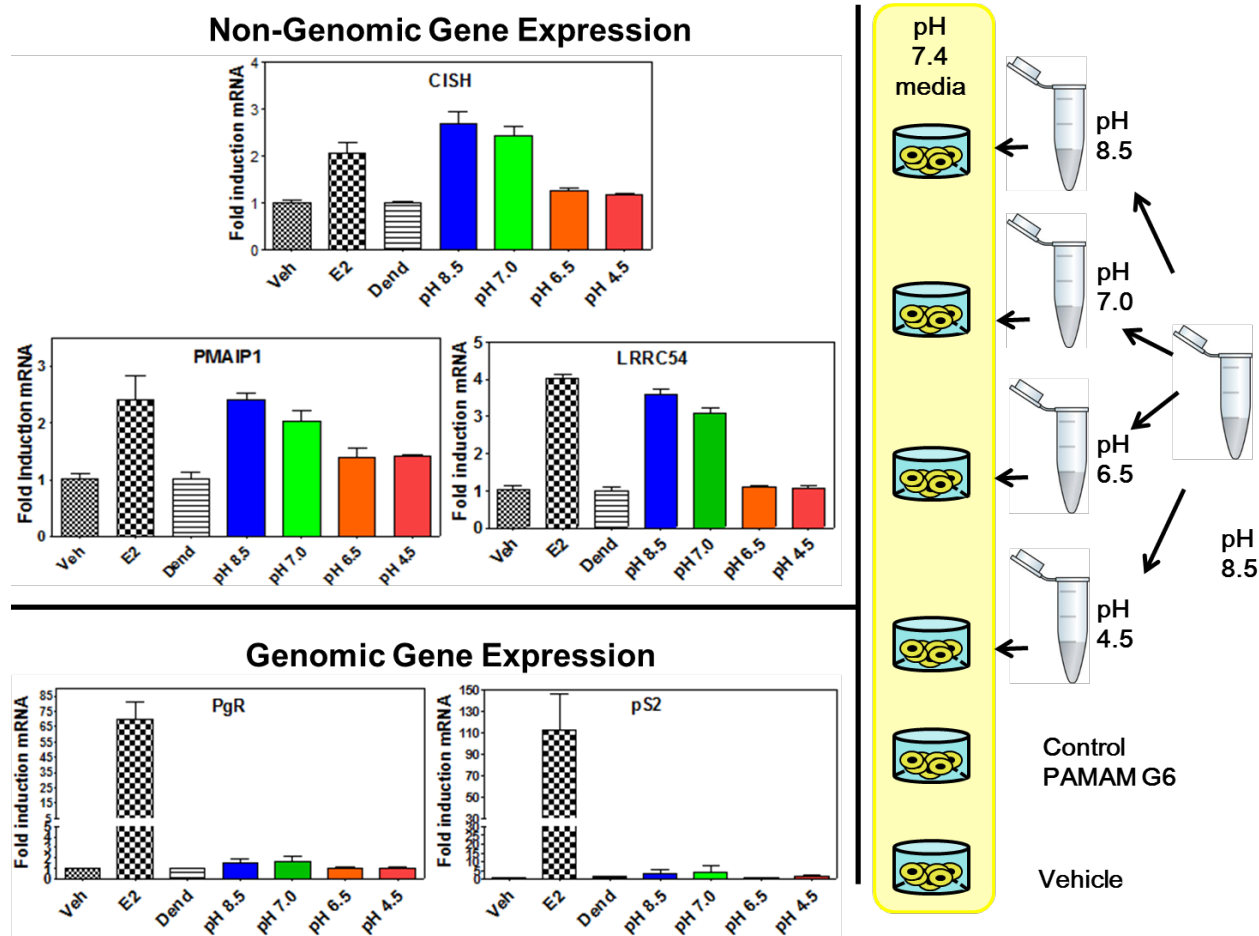


**Figure 4.** Gene expression in MCF-7 cells treated with 10 nM E<sub>2</sub> or 10 nM E<sub>2</sub>-equivalent of EDC. The non-genomic genes, CISH, PMAIP1, and LRRC54 (top), can be stimulated by estrogen receptor acting at extra-nuclear sites; so both E<sub>2</sub> and EDC are active. The genomic genes, PgR and pS2 can be stimulated only by nuclear activity of the estrogen receptor (bottom), so only E<sub>2</sub> is active. (Veh: vehicle treated control cells, E2: Estradiol (10 nM) treated cells, Dend: Underivatized Control G6 PAMAM dendrimer treated cells, pH 8.5, 7.0, 6.5, and 4.5: Cells treated with EDC samples that had been exposed to different pH conditions.

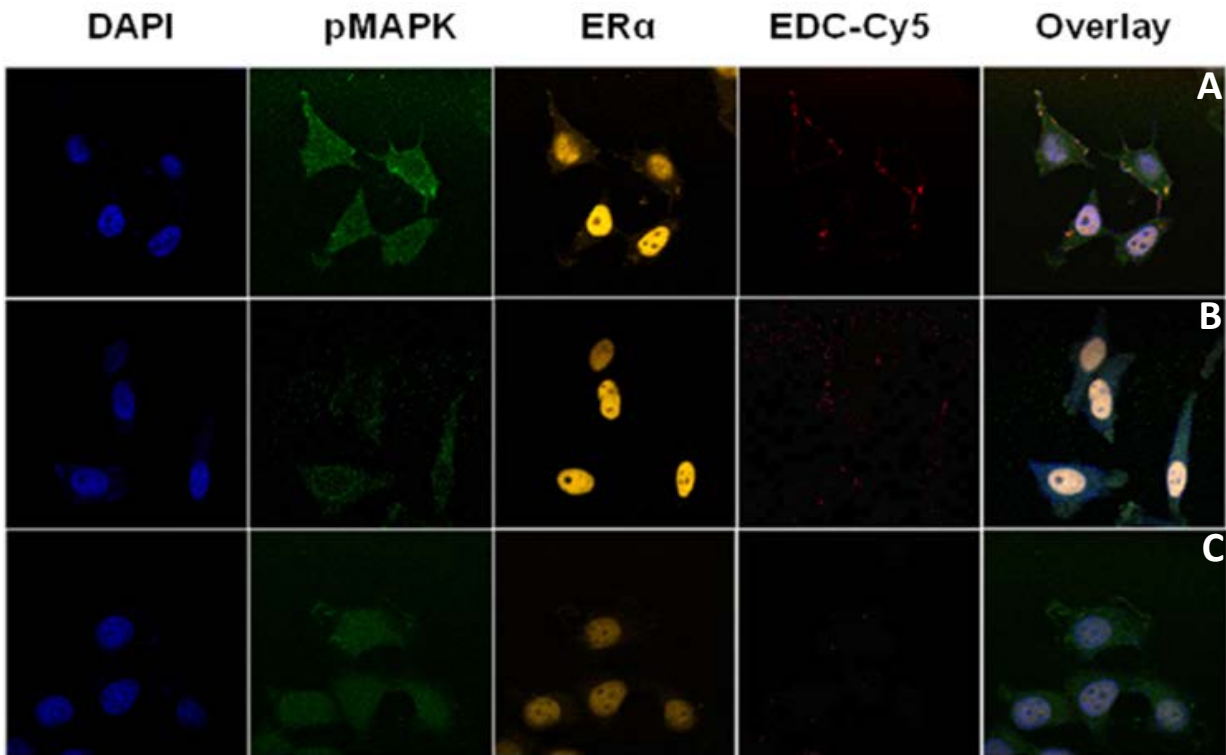


**Figure 5. Multicolor fluorescence microscopic imaging to visualize the colocalization of Cy5-labeled EDC (Cy5-EDC), ER $\alpha$ , and pMAPK. A.** Colocalization of Cy5-EDC maintained at pH 8.5. Cy5-EDC (red), ER $\alpha$  (Alexa-568, yellow), and pMAPK (Alexa-488, green). **B.** Colocalization of Cy5-EDC exposed to pH 6.5. **C.** Colocalization of control Cy5-PAMAM G6 control dendrimer compound maintained at pH 8.5. Each EDC was incubated at 1  $\mu$ M (ligand equivalent) with MCF-7 cells for 15 min at 37  $^{\circ}$ C for images A, B. Cy5-PAMAM G6 dendrimer at 50 nM was treated to get image C. The same amounts of ER $\alpha$  and pMAPK antibody were used as in A, B, C to get image D. ER $\alpha$  and pMAPK antibody were labeled with Alexa-568 and Alexa-488, respectively. Columns (left to right) display the location of the nuclei (DAPI), pMAPK, ER $\alpha$ , EDC, and an overlay, respectively. All images were taken at 60x magnification.



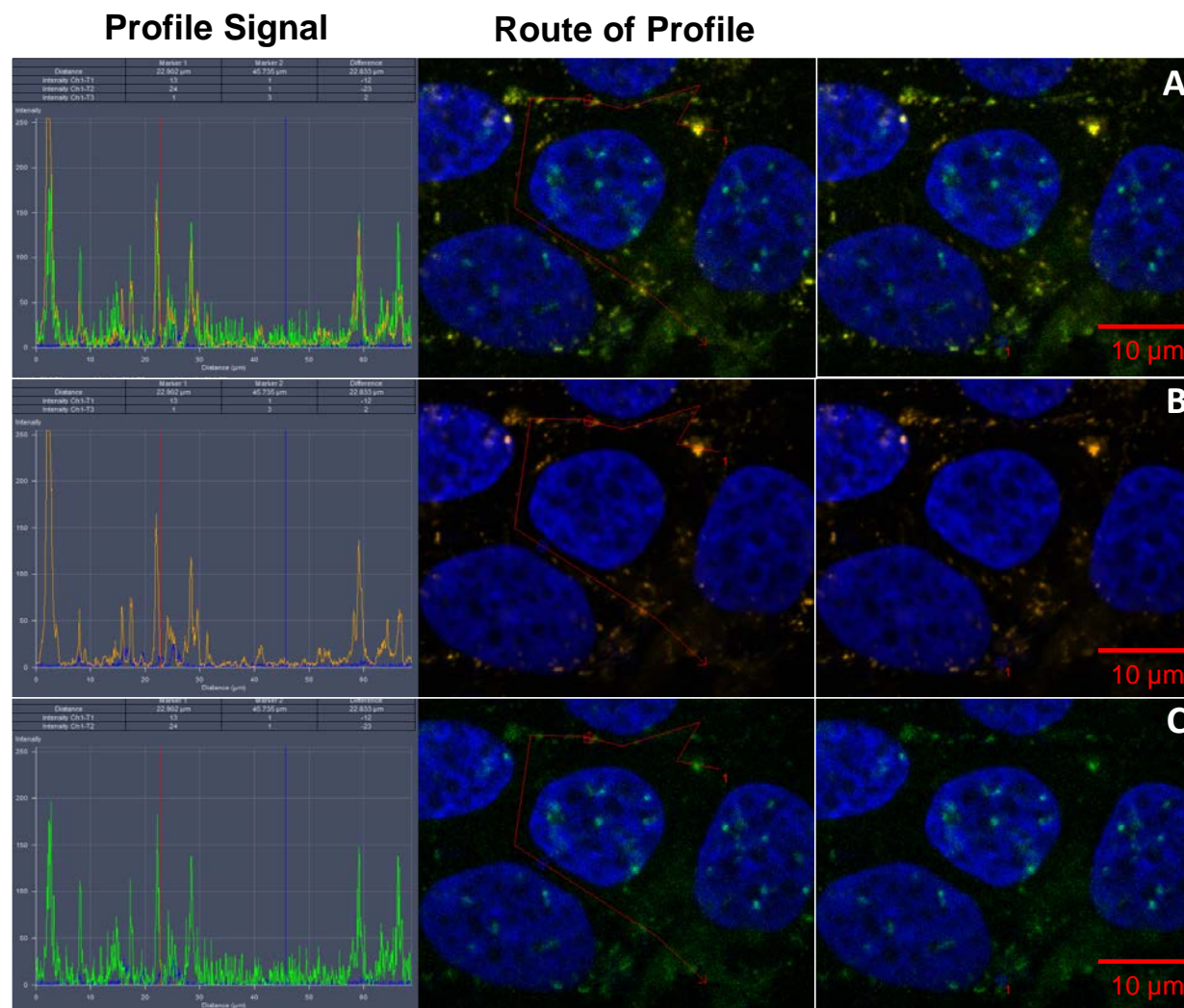


**Figure 6. Confocal microscopic imaging for proximity ligation assay (PLA).** PLA highlights the close interaction among ER $\alpha$ , pMAPK and EDC-TMR in the extra-nuclear cellular area, thought to result in the initiation of kinase-cascade signal transduction. The x-axis of the histograms (*left column*) indicates signal intensity at the corresponding location along the red-line track drawn in the picture (*right column*). Top row (A) shows the overlaid microscopic image of EDC-TMR (red), DAPI (blue; nucleus), and the PLA signal from the ER $\alpha$  and pMAPK complex (green). The middle (B) and bottom (C) rows illustrate the localization of EDC-TMR and the proximity-ligated ER $\alpha$  and pMAPK complex (ER $\alpha$ -pMAPK PLA complex), respectively. TMR-

EDC maintained at pH 8.5 as prepared was added to MCF-7 cells for 45 min, and the PLA assay was performed.

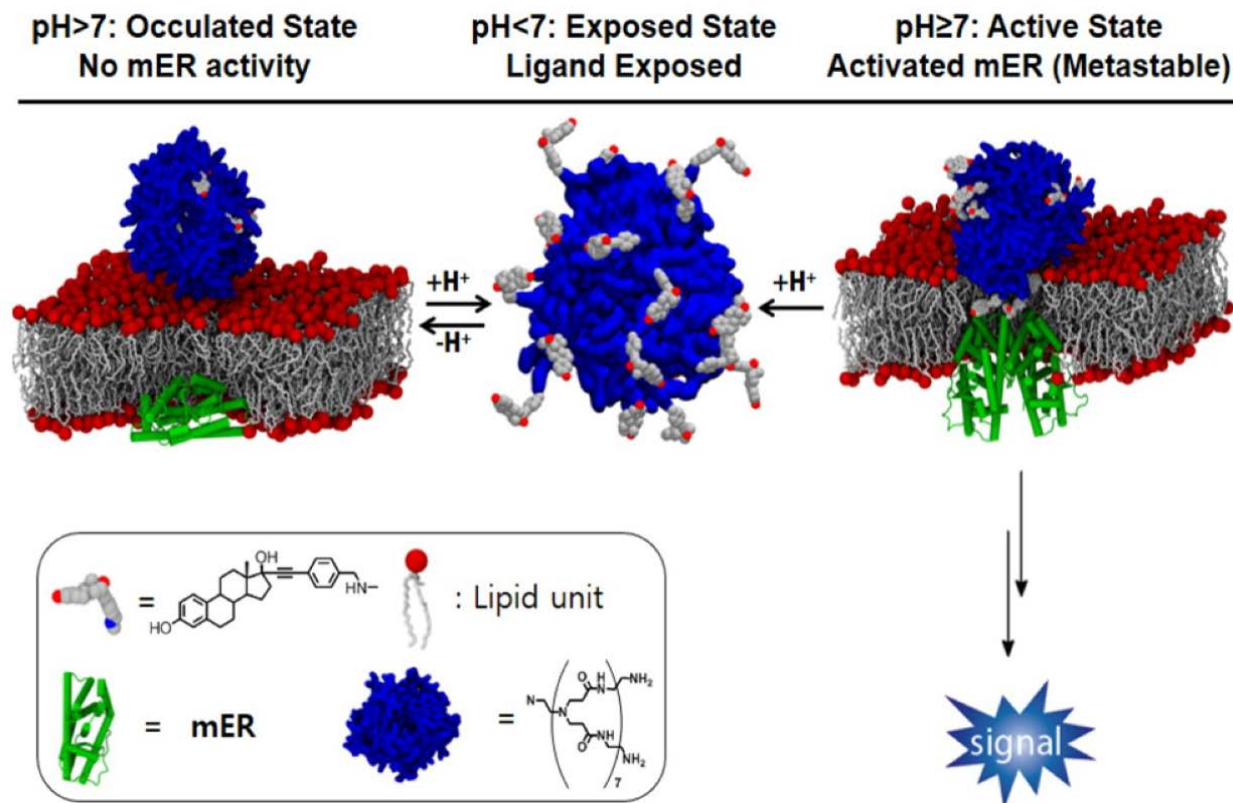


**Figure 7. Schematic representation of the three states of the EDC and interaction with membrane ER (mER) and a membrane bilayer.** The “Surface-Compact State” (*right*) is the active, but metastable form produced only during EDC synthesis at pH 8.5. In this state the ligands are held close to the surface of the surface-compact form of the PAMAM dendrimer, and they display some mobility, experience limited fluorescence quenching, and can be accessed by the fraction of estrogen receptors that controls non-genomic gene expression (designated as membrane ER or mER). The “Expanded State” of the EDC (*middle*), which forms at low pH (4, 6.5), extends the ligands, giving them mobility and exposing them to active quenching, but cell activity cannot be assayed at these acidic pH values. Returning the expanded state to pH 7.4 for cell-based assays results in a transition to the “Occluded State” (*left*), more stable than the surface-compact state, in which the lipophilic ligands become entrapped in the more lipophilic interior of the PAMAM dendrimer and cannot be accessed by the mER. (All three elements, EDC, membrane, and mER (ligand binding domain) were generated by molecular modeling and are represented at relative scale in the left and right images. Details on modeling and skeletal representations of EDC and DPA-DC are given in **Figures 1** and Supplementary Information **S1**)



